JOURNAL OF PROPULSION AND POWER
Vol. 18, No. 3, May–June 2002

Technical Notes

TECHNICAL NOTES are short manuscripts describing new developments or important results of a preliminary nature. These Notes cannot exceed 6 manuscript pages and 3 figures; a page of text may be substituted for a figure and vice versa. After informal review by the editors, they may be published within a few months of the date of receipt. Style requirements are the same as for regular contributions (see inside back cover).

Geometric Evaluation of Axisymmetric Thrust-Vectoring Nozzles for Aerodynamic Performance Predictions

Erich A. Wilson,* Dan Adler,† and Pinhas Z. Bar-Yoseph‡
Technion—Israel Institute of Technology, 32000 Haifa, Israel

Nomenclature

A	=	area, m^2
A_e^j/A_t^j	=	nozzle area control ratio @ $j = E, G$
CD	=	flow coefficient at the nozzle throat
M	=	Mach
r	=	radius, m
V_c	=	effective nozzle expansion volume, m^3
W	=	gas flow rate, kg/s
x	=	nozzle expansion length, m
x_n	=	length of divergent nozzle flaps, m; $x_G/\cos\alpha$ @ $\delta_{\mathrm{Gy},z} = 0$
α	=	nozzle divergence angle, rad
β	=	nozzle convergence angle, rad
δ	=	nozzle jet deflection angle, rad
ξ	=	one-dimensional radial elongation of r_t^E

Subscripts

c	=	control constant
E	=	effective
e	=	exit
G	=	geometric
i	=	variable (yaw or pitch)
t	=	throat
x	=	body-axis direction
y	=	yaw direction
z	=	pitch direction
7	=	nozzle entrance station number
8	=	nozzle throat station number
$\perp$	=	normal to A_t^G

Superscript

j	=	variable (effective or geometric)

Introduction

JET deflection to obtain forces for enhancing aircraft performances is the aim of thrust-vectoring (TV) technology. In military aircraft[1] it has been proven to greatly increase aircraft maneuverability in the pitch roll and yaw directions. This includes the capability of taking the aircraft into high-angle-of-attackmaneuver. It has also been proven to increase fighter kill ratio and survivability. In civil aircraft[2] it has been documented to increase aircraft safety and maneuverability through providing control recovery in such emergency situations as microbursts, engine failure, and loss of lift, among others. In general, it allows for the use of shorter runways through the added capability of short takeoffs and landings.

TV aircraft flight control is obtained through the addition of new hardware to extant aircraft or through the incorporation of TV flight control into current and future design processes. In the military domain the X-31, F-22, Su-37, F-18, F15, and F-16 programs, among others, have demonstrated this technology. In the civil and transport jet domain TV has yet to be fully researched and implemented.

To establish the benefits extractable from particular hardware, an explicit method to calculate TV nozzle performance capabilities is needed in both the fixed- and variable-geometry TV configurations. Analytical definitions for the variable geometry of axisymmetric and two-dimensional converging–diverging TV nozzles have been offered in part by some authors.[3–7] These authors define the general geometrical differences between conventional and dynamic TV nozzles. Detailed numerical TV modeling studies that demonstrated the capability of using computational fluid dynamics (CFD) as a viable design tool in TV nozzle modeling were pursued by Carlson[8] and Matesanz and Velaquez.[9]

The effects of nozzle geometry on the jet flow are assumed by Decher[10] to be a basic component to nozzle design. This conclusion is further supported by Persen et al.[11] who conclude from their experimental investigations that values such as the nozzle shape and outlet diameter are fundamentally important governing parameters. These determine the behavior of the jet flow after exiting the nozzle under static conditions. Persen et al. further assert that the nozzle geometry exclusively governs the jet flow behavior for a fixed nozzle pressure ratio (NPR). So, clearly, any analytical TV nozzle model must be based on correct definitions of the dynamic TV geometry.

Once the geometry is properly defined, the internal fluid mechanics can be approached. Matesanz and Velaquez[9] establish the variation of nozzle performance (i.e., of flow geometry and flow direction variation) as a function of the NPR for a given converging-diverging axisymmetric nozzle configuration.

The most thorough numerical investigation into the modeling of TV nozzle is performed by Carlson.[8] He presents a numerical internal nozzle performance prediction algorithm for paddle-type TV nozzles as found on the F-18 HARV and the X-31. Using three-dimensional Navier–Stokes equations, four different case studies are supplied to validate the method. Precision in matching the experimental data for the thrust coefficient within experimental accuracy is achieved with similarly excellent results for the moment and force ratios.

In axisymmetric TV nozzles rotated at the throat (i.e., throat-hinged), vectoring alters the exit geometry from circular to quasi-elliptic in cross section. This phenomenon is not reviewed here. Though, geometric similarity is provided in the basic patterns of elliptic flow such as that given in brief by Elangovan et al.[12]

This study seeks to define completely the basic dynamic geometry of thrust-vectoring nozzles rotated at their throat. To this end, an explicit analytical algorithm for calculating the nozzle geometry during vectoring is presented. Distinctions are made between the

Received 25 August 1999; revision received 11 June 2001; accepted for publication 25 June 2001.

*Graduate Student.
†Professor and Head of the Turbomachinery Laboratory.
‡Professor and Head of the Computational Mechanics Laboratory.

dynamic geometry of the effective expansion volume of the nozzle. The capability of using these geometrical metrics to predict the effective vectoring angle is validated and described through comparison with experimental data. This study is pursued at constant NPR and the ground conditions of zero Mach and zero altitude, nullifying flight velocity effects on the jet flow.

This explicit TV nozzle geometrics algorithm can be used in future TV nozzle design procedures for refining and reducing costly experimental investigations. Further, it can be implemented to evaluate current TV nozzle performance capabilities that may not be known to enhance aircraft and defense simulations. In the civil and transport aircraft domain this algorithm can be used in design and simulation of extractable TV performances in convergent nozzles through allowing the nozzle area ratio to be unity.

Mathematical Formulation

Dynamic TV Nozzle Control Definitions

During thrust vectoring, the nozzle control ratio A_e/A_t is maintained either as a function of the effective nozzle area ratio A_e^E/A_t^E or as a function of the geometric nozzle area ratio A_e^G/A_t^G. Under the variable-geometry control the effective nozzle area ratio A_e^E/A_t^E is maintained constant throughout vectoring while the geometric nozzle areas are forced to increase in compensation to maintain constant thrust over the vectoring range.

The geometric definitions of TV nozzles are given in Fig. 1. Although the effective length x_E is reduced as the nozzle opens, the effective expansion volume of the nozzle remains unchanged through a proportional increase in the nozzle divergence angle. Thus, the effective nozzle x–y and x–z planar areas ($\perp A_{cy}$, $\perp A_{cz}$) normal to A_t^G, which are equal in conventional axisymmetric nozzles. Thus, one can define the effective nozzle expansion volume V_c such that it remains constant throughout vectoring and serves as a basis for the geometric planar areas. These definitions will serve as control concepts for calculating the nozzle geometry in vectored positions.

Under fixed-area control the opposite process occurs: the geometric nozzle area ratio A_e^G/A_t^G is maintained constant throughout vectoring while the effective nozzle areas are forced to decrease. Thus, the geometric nozzle x–y and x–z planar areas and volume ($\perp A_{cy}$, $\perp A_{cz}$, V_c) remain constant throughout vectoring. The jet becomes increasingly underexpanded proportional to the deflection angle. In supersonic flow this is accompanied by a proportional decrease in thrust. It has been shown, however, that this scenario actually provides an increase of thrust in subsonic flow.[13]

The algorithm presented in this work is specifically intended for both fixed-and variable-geometry axisymmetric converging–diverging TV nozzles. It is also applicable to the two-dimensional nozzles through a minor geometrical transformation. Further, this can be applied to converging nozzles in civil and transport aircraft when the area control ratio is forced to unity and controlled by the vectoring flap geometry.

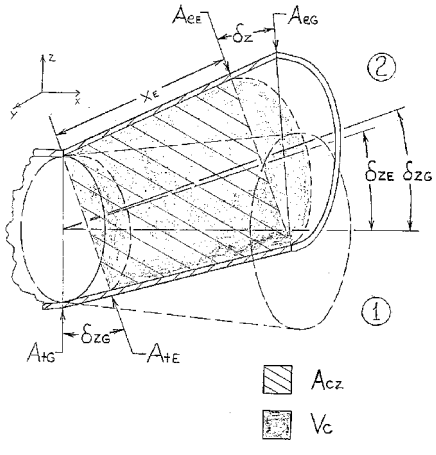

Fig. 1 Schematic two-dimensional representation of a pitch-up nozzle command.

Calculating for a Fixed-Area TV Nozzle

To clarify the control concept, define the control area and control volume ($\perp A_c$, V_c,) where the areas in the x–y and x–z planes are identical by symmetry in this example. Then, for the variable-area ($j = E$) and fixed-area ($j = G$) such that

$$\perp A_{ci} = \perp A_t^j, \qquad \perp A_{ci} = x \int_{-r_t}^{r^e} dr = \left(r_{ti}^j + r_{ei}^j\right)x$$

$$V_c = \frac{1}{8x}\int_0^{\perp A_{ci}}\int_0^{2\pi} A\partial\theta\partial A = \frac{A_t^j + A_e^j}{2}x, \qquad \text{at } i = y, z \quad (1)$$

where the nozzle expansion length x is the effective expansion length x_E under variable-area control (defined next). The nozzle expansion length x for fixed-area nozzle control is variable conforming to $x = x^G \cos\delta_z^G \cos\delta_y^G$, with x_G as the nozzle expansion length with no vectoring and δ_z^G and δ_y^G as the geometric pitch and yaw vectoring angles, respectively.

The effective nozzle throat area A_t^E including nozzle divergence is assumed to remain fixed to the geometric nozzle throat area A_t^G at one point, even though in reality this is not always the case. Thus, define the geometric relation for the radial extension of the effective throat area into the nozzle divergent sector in one dimension (pitch or yaw)

$$\xi_i = \left(\cos\delta_i^G + \sin\delta_i^G \tan\alpha_i\right) \quad (2)$$

where $i = y, z$, and α_i, the planar average nozzle divergence angle assumed uniform in the respective x–y or x–z plane. Making considerations from this point on for coupled pitch and yaw movements of the nozzle, the nozzle geometric throat radii and the average effective throat radii are related by

$$r_{t_i}^E = r_t^G\left(\xi_i + \sin\delta_j^G \tan^2\alpha_j\right) \quad (3)$$

where $i = z$, y and $j = y$, z, respectively. As $\delta_j^G > 0$, the effective throat shifts into the divergent sector of the nozzle while the jet flow conforms to the dynamic elliptic geometry of the nozzle. This geometric-effective throat-area relation (see Fig. 1) is written

$$A_t^E = A_t^G\left(\xi_z + \sin\delta_y^G \tan^2\alpha_y\right)\left(\xi_y + \sin\delta_z^G \tan^2\alpha_z\right) \quad (4)$$

an expansion from the preceding simplified relation of $A_t^E = A_t^G \cos\delta_y^G \cos\delta_z^G$ (see Refs. 3–6). Assuming that the exit-area deviation from orthogonality with the divergent nozzle centerline is negligible, the effective expansion length is approximated as

$$x^E = x^G - 2r_t^G\left(\sin\delta_z^G + \sin\delta_y^G\right) \quad (5)$$

In this scenario the planar control area is the constant geometric planar area from Eq. (3). Thus, the elliptic geometric exit radii are found:

$$r_{e_z}^G = \frac{A_c}{x^E} - r_t^G, \qquad r_{e_y}^G = \frac{A_t^G\left(A_e^G/A_t^G\right)}{\pi r_{e_z}^G} \quad (6)$$

and the orthogonal planar average nozzle divergence angle is

$$\alpha_i = \arctan\left(\frac{r_{ei}^G - r_t^G}{x^E}\right), \qquad \text{at } i = y, z \quad (7)$$

The effective exit radii become

$$r_{e_i}^E = r_{t_i}^E + x^E \tan(\alpha_i), \qquad \text{at } i = y, z \quad (8)$$

while the effective exit area in this scenario is found through the relation $A_e^E = \pi r_y^E r_z^E$. For the variable-nozzle calculations Eqs. (6–8) would simply switch the effective subscript for the geometric subscript and vice versa. For convergent TV nozzles the nozzle area ratio is unity unless changed by a quasi-divergent sector of TV flaps opening.

Aerodynamic Nozzle Performances

The geometry for a dynamic axisymmetric nozzle during thrust vectoring has now been defined. The relevance of the geometrical influence on the internal fluid mechanics of a nozzle was established earlier. Thus, the relation in this work between geometry and fluid mechanics can now be clarified.

The inability to determine the precise flow characteristics that are functions of the pressure and temperature of the flow from the nozzle geometry is clear. Yet, the geometrical configuration of the nozzle can provide an upper bound to the effective vectoring angle of the flow. This is possible through the preceding definition of the effective nozzle throat and exit angles, assuming that the highest effective vectoring angle as a function of NPR at a constant geometric vectoring angle coincides with the presence of an oblique shock in the nozzle. Then, the shock that forms in the nozzle is estimated to be radially parallel to the effective nozzle exit area. In such a case the flow can be assumed to exit normal to that shock as an upper limit for the possible effective vectoring angle.

The angular difference between the effective and geometric areas at the nozzle exit thus determines an upper bound of the effective vectoring angle. This relation for the effective vectoring angle prediction is

$$\delta_i = \arccos\left(r_{e_i}^E \big/ r_{e_i}^G\right), \qquad \text{at } i = y, z \tag{9}$$

The flow coefficient was already proposed to simply be the ratio between the effective and geometric throat areas.[3] However, that assumption is improved when the flow coefficient is a simple adjustment to the conventional unvectored value as a function of the effective throat area

$$C_{D8} = \frac{M_{7\text{actual}}}{M_{8\text{ideal}}} \cong \frac{A_{tE}}{A_{tG}}\left(C_{D8}|_{\delta_G=0}\right) \tag{10}$$

In this work the conventional flow coefficient is taken from the proposed fit of Berrier and Re,[14] which is given as

$$C_{D8}|_{\delta_G=0} = 1.0 - \tfrac{1}{2}(1.0 - \cos\beta) \tag{11}$$

where β is the convergent nozzle angle before the throat.

Data Theory Comparison

Applying the preceding mathematical formulation in four cases to the metrics of two fixed-area axisymmetric thrust-vectoring nozzle configurations, see Ref. 15, and comparing the resulting predictions with the experimental data gives greater insight to the accuracy expected from the theory. The two configurations consist of a long-flap nozzle close to the ideal expansion length and a short-flap nozzle. Both are operated in dry-thrust and afterburner modes. The throat areas of the dry-power unvectored nozzles are $A_t = 0.0026\,\text{m}^2$ and $0.0048\,\text{m}^2$ for the afterburning configurations. Each nozzle has a conventional area ratio of $A_e/A_t = 1.35$, whereas the flap length for the long nozzle configuration is $x_G = 0.0760$ m and 0.0506 m for the short nozzle configuration.

With the inputs just listed for the unvectored nozzle position, Eq. (1) is used to first calculate the planar control area and the control volume for each case, as listed in Table 1. With these controls established, Eqs. (2–11) are applied to calculate the algorithmic prediction performance.

The predictive calculations are given for case 1, Figs. 2, 3; case 2, Figs. 4–6; case 3, Fig. 7; and case 4, Figs. 8, 9. It can be seen that

Table 1 Calculated planar control area and control volume for each case

Case	A_c, m^2	V_c, m^3
Dry (long)	0.02967	0.009144
Dry (short)	0.01975	0.006088
AB (long)	0.04038	0.016960
AB (short)	0.02682	0.011260

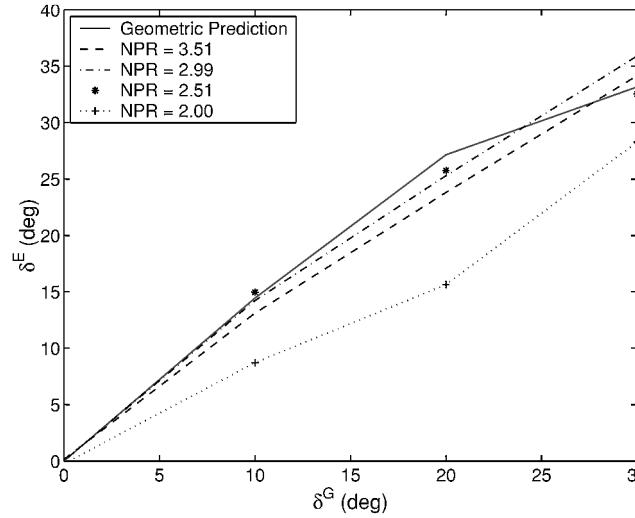

Fig. 2 Case 1 effective vs geometric vectoring angle.

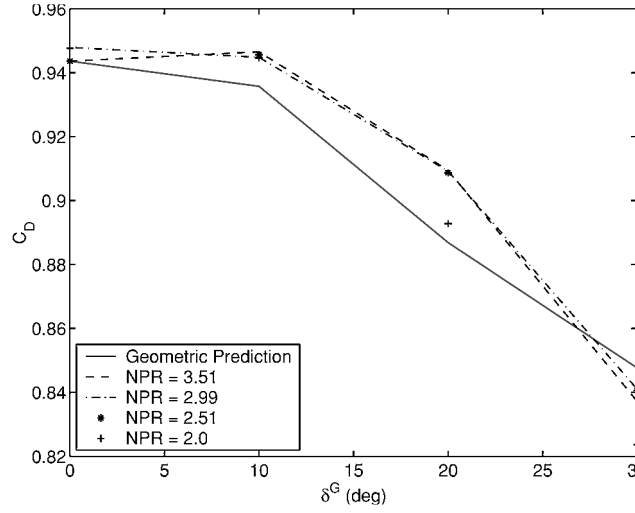

Fig. 3 Case 1 flow coefficient vs geometric vectoring angle.

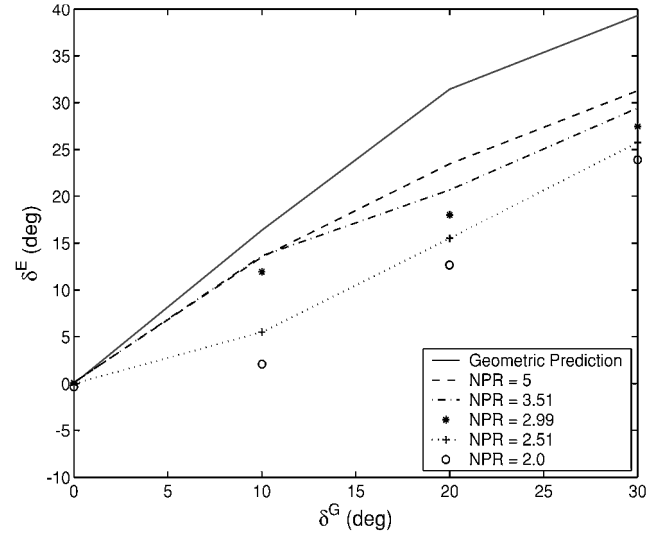

Fig. 4 Case 2 geometric vs effective vectoring angle.

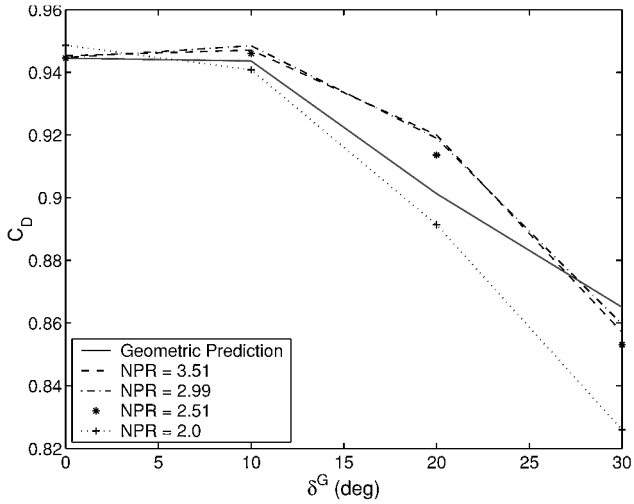

Fig. 5 Case 2 flow coefficient vs geometric vectoring angle.

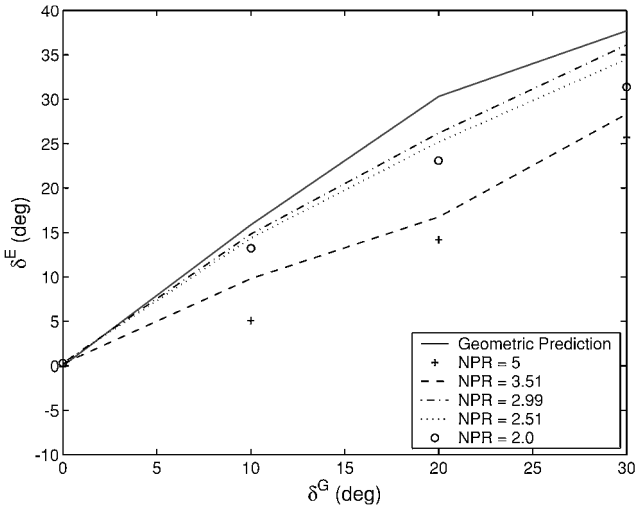

Fig. 6 Case 2 geometric vs effective vectoring angle.

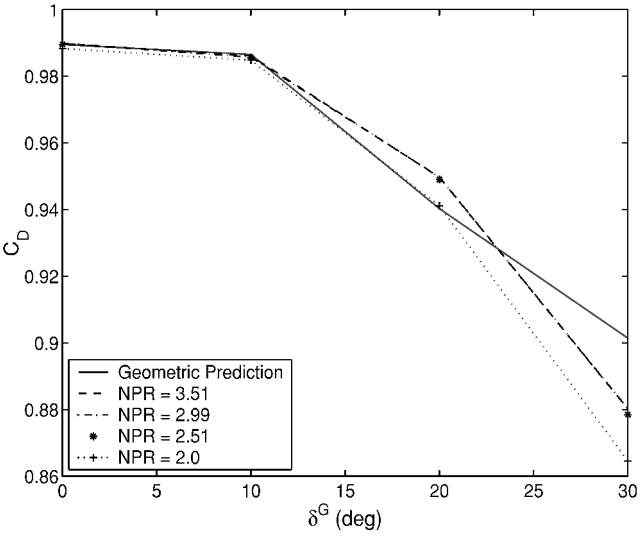

Fig. 7 Case 3 flow coefficient vs geometric vectoring angle.

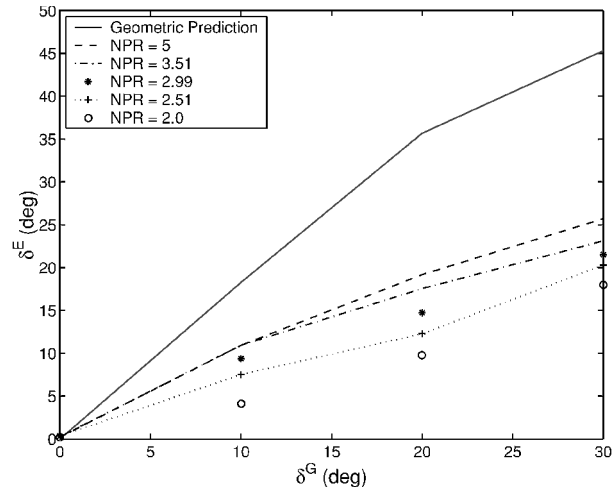

Fig. 8 Case 4 geometric vs effective vectoring angle.

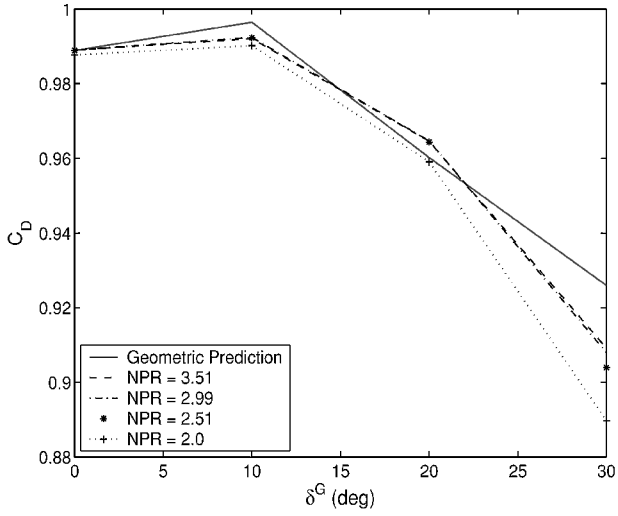

Fig. 9 Case 4 flow coefficient vs geometric vectoring angle.

for each case, Figs. 2, 4, 6, and 8, a peak effective vectoring angle exists at a specific NPR. This is referred to as the NPR peak performance point and is closely matched by the performance prediction algorithm presented here.

The effective vectoring angle is best predicted in case 1, Figs. 2 and 3, which is the most ideal case of a nonafterburning nozzle with long flaps. Of course, of the four cases this most resembles the Laval nozzle. Subsequently, when the nozzle flaps are shortened in case 2, Figs. 4 and 5, the geometric prediction is less effective as a result of the increased sensitivity of the nozzle performances on the larger nozzle divergence angle. This sensitivity is not taken into account in this work. When placed at the same NPR peak performance location as case 1, Fig. 6, it is quite apparent that the prediction does not match the data.

The effects of afterburning, or rather a large increase in area to accommodate afterburning, tend to decrease the precision of the geometric prediction slightly. Thus, its effects are visible in cases 3 and 4, although the prediction remains reasonable.

The flow coefficient prediction does not vary significantly for any of the models and is a generally good model for all cases. This algorithm is entirely independent of NPR, and when graphed with it is chosen at locations to simply match the NPR peak performance of the effective vectoring angle.

Conclusions

An explicit calculation procedure for the dynamic geometry of TV nozzles was presented. Relation of the geometry to the flow performances was elaborated and used to create a model for determining the flow coefficient and a maximum effective vectoring angle. This model was then compared with experimental data. The geometric predictions compared proved to be able to predict the upper bound of the effective vectoring angle very well, whereas the geometry only was proven to describe the variation in the flow coefficient with vectoring, but not the conventional flow coefficient.

Though the prediction decreased in precision with the addition of afterburning, it remains within experimental accuracy. As the flaps on the nozzle were shortened, the prediction diverged from the nozzle data as a function of vectoring angle, proving the dependence of jet performance on the nozzle divergence angle. In other words, the greater the divergence angle, the less ideal the jet expansion. Thus, the geometrical predictions have been verified for quasi-ideal cases and can be used in future TV nozzle design to reduce costly experimental investigations.

Further, it may be implemented to evaluate current TV nozzle performances to enhance aircraft and defense simulations, as well as provide realistic initial conditions for future numerical vertical/standard takeoff and landing/TV jet performance studies. In the future NPR influence on nozzle performance may be included in this procedure for a more robust nozzle performance prediction across the NPR range.

References

[1]Mace, J., Smereczniak, P., Krekeler, G., Bowers, D., MacLean, M., and Thayer, E., "Advanced Thrust Vectoring Nozzles for Supercruise Fighter Aircraft," AIAA Paper 89-2816, 1989.

[2]Burken, J., Burcham, F., Maine, T., Feather, J., Goldthorpe, S., and Kahler, J., "Flight Test of a Propulsion-Based Emergency Control System on the MD-11 Airplane with Emphasis on the Lateral Axis," NASA-TM-4746, July 1996.

[3]Gal-Or, B., "Complete Thrust Vectoring Flight Control for Future Civil Jets, F-22 Superiority Fighter and Cruise Missiles. Part I: Vectored F-22, F-16 and F-15," *International Journal of Turbo and Jet Engines*, 10, 1993, pp. 1–17.

[4]Gal-Or, B., "Fundamental Concepts of Vectored Propulsion," *Journal of Propulsion and Power*, Vol. 6, No. 6, 1990, p. 747.

[5]Gal-Or, B., *Vectored Propulsion Supermaneuverability and Robot Aircraft*, Berlin, Springer-Verlag, 1991, pp. 1–294.

[6]Wilson, E., "A Two-Spool Turbofan Thrust Vectoring Analysis," M.Sc. Thesis, Technion—Israel Inst. of Technology, Haifa, Israel, Faculty of Mech. Engineering, July 1997.

[7]Matesanz, A., Velaquez, A., and Rodriguez, M., "Aerodynamic Prediction of Thrust-Vectoring Nozzles," *Journal of Propulsion and Power*, Vol. 14, No. 2, 1998, pp. 241–246.

[8]Carlson, John R., "A Nozzle Internal Performance Prediction Method," NASA-TP-3211, Oct. 1992.

[9]Matesanz, A., and Velaquez, A., "Performance Analysis of an Axisymmetric Thrust Vectoring Nozzle Using the FUNSIF3D Code," AIAA Paper 95-2743, June 1995.

[10]Decher, R., "Mass Flow and Thrust Performance of Nozzles with Mixed and Unmixed Nonuniform Flow," *Journal of Fluids Engineering*, 117, Dec. 1995, pp. 617–622.

[11]Persen, L. N., Oiann, H., and Mazumdar, H. P., "The Round Thermal Jet: Undisturbed and in a Crossflow," *International Journal Heat and Mass Transfer*, Vol. 36, No. 6, 1993, pp. 1598, 1599.

[12]Elangovan, S., Solaiappan, A., and Rathakrishnan, E., "Studies on Twin Elliptic Jets," *Aeronautical Journal*, Vol. 100, No. 997, 1996, pp. 295, 296.

[13]Wilson, E., Adler, D., Gal-Or, B., Sherbaum, V., and Lichtsinder, M., "Optimizing Subcritical-Flow Thrust-Vectoring of Converging-Diverging Nozzles," *Journal of Propulsion and Power*, Vol. 16, No. 2, 2000, pp. 202–206.

[14]Berrier, B. L., and Re, R. J., "Investigation of Convergent-Divergent Nozzles Applicable to Reduced-Power Supersonic Aircraft," NASA-TP-1766, 1980.

[15]Carson, G. T., and Capone, F. J., "Static Internal Performance of an Axisymmetric Nozzle with Multiaxis Thrust-Vectoring Capability," NASA-TM-4237, Feb. 1991.

Combustion Characteristics of Ethylene in Scramjet Engines

A. A. Taha,* S. N. Tiwari,† and T. O. Mohieldin‡
Old Dominion University, Norfolk, Virginia 23529

Introduction

MOST of the scramjet combustion studies, currently being conducted, use liquid hydrocarbon fuels or hydrogen. The use of hydrocarbon fuels in volume-limited systems will require an ignitor and some form of combustion enhancement.[1] The results of the early tests conducted by Kay et al.[2,3] clearly demonstrated that the supersonic combustion of various hydrocarbon fuels could be achieved; although for many test conditions special externally mounted piloting devices were required to initiate and stabilize the flame.

The piloted-supersonic combustion experiments strongly recommended that hydrogen piloting is highly effective for a variety of fuels including methane and kerosene. A monopropellent, OTTO fuel, was successfully used as an effective pilot in the scramjets.[1] Other results showed that silane/hydrogen mixtures were effective pilots for ethylene and kerosene combustion.[4]

Ethylene C_2H_4 is a primary fuel itself and is also produced in large amounts during the combustion of methane CH_4, ethane C_2H_6, and other higher hydrocarbons.[5] Ethylene is often chosen for the hydrocarbon-fueled scramjet engines tests because it is used as a surrogate test fuel for hydrocarbon fuels.

The intent of this study is to investigate the supersonic combustion flowfield of ethylene as a candidate hydrocarbon fuel in scramjet engines. Special attention is paid to studying the effect of piloting on the main flame initialization and stabilization. During this phase of the study, piloting with gaseous ethylene was used while the proposed objective is to use hydrogen as a pilot fuel. Because of the unavailability of experimental data for the supersonic combustion of ethylene, the verification of the present numerical results with existing experimental results could not be achieved. Therefore, the validation of the computational fluid dynamics (CFD) Fluent code[6] was achieved by comparing cold-flow numerical results with the pertinent experimental results of McDaniel et al.[7] This verification study was published in Ref. 8

Theoretical Model and Computational Procedure

The schematic diagram for the configuration used in the present study is presented in Fig. 1 in which a rearward-facing step is located at the upper longitudinal wall. Sonic pilot ethylene is injected parallel to the incoming airstream via three 1-mm circular holes that are equally distributed at the base of the step. The pilot ethylene static temperature is 500 K with equivalence ratio of 0.06 calculated based on the mass flow rate of the incoming supersonic air inlet. The inflow is vitiated air with Mach number = 1.756 to simulate the enthalpy level of the typical conditions at the combustor inlet. The total temperature is 1800 K while the total pressure is set to be 431.762 kPa. The vitiated supersonic air inlet contains H_2O with mass fraction of 0.17. A 15-deg wedge is located downstream of the step and upstream of the main normal injection. The combination

Received 5 January 2001; revision received 10 September 2001; accepted for publication 10 December 2001.

*Graduate Research Assistant, Department of Mechanical Engineering, College of Engineering and Technology. Student Member AIAA.

†Eminent Professor/Scholar, Department of Mechanical Engineering, College of Engineering and Technology. Associate Fellow AIAA.

‡Professor, Mechanical Engineering Technology Department, College of Engineering and Technology.